

Production of hypernuclei in a 2.1 GeV/nucleon oxygen beam*

K. J. Nield, † T. Bowen, G. D. Cable, ‡ D. A. DeLise, E. W. Jenkins,
R. M. Kalbach, R. C. Noggle, and A. E. Pifer

Department of Physics, University of Arizona, Tucson, Arizona 85721

(Received 9 October 1975)

The first hypernuclei production experiment using a beam of heavy ions from the Lawrence Berkeley Laboratory Bevatron is described. Mass 16 hypernuclei were produced by 2.1 GeV/nucleon ^{16}O ions incident on a polyethylene target. These relativistic hypernuclei were studied with large gap spark chambers that were electronically triggered by the low momentum K^+ meson produced in association. Analysis of 22 events yields a mean lifetime $\tau(^{16}\Lambda) = (0.86^{+0.33}_{-0.26}) \times 10^{-10}$ sec.

NUCLEAR REACTIONS Hypernuclei ($^{16}\text{O}, ^{16}\text{N}_\Lambda$ or $^{16}\text{O}_\Lambda$) K^+ , $E = 2.1$ GeV/nucleon, polyethylene target, σ_t roughly measured; mean lifetime of mass 16 hypernuclei measured.

Since relativistic hypernuclei might travel many centimeters in the laboratory before decaying, they could escape from thick production targets and their lifetimes could be readily observed. Relativistic velocity also would facilitate measuring Z of the hypernucleus, and decay products would be contained within a small laboratory solid angle suitable for momentum analysis.

A search was made in a 2.1 GeV/nucleon ^{16}O beam¹ at the Lawrence Berkeley Laboratory Bevatron for relativistic hypernuclei associated with the production of low momentum K^+ mesons which provide an electronic signature by their delayed decay after stopping. A beam intensity of $\sim 3 \times 10^5$ ^{16}O ions/pulse with approximately a 1 sec beam spill were focused such that 90% of the particles were within a 1.25 cm diameter beam spot size. Figure 1 illustrates the counters and spark chambers used in the experiment. The counter logic was based upon (a) signal B to detect an interaction in the target caused by an on-axis beam particle, and (b) signal K to denote detection of charged decay products of the K^+ . These signals were

$$B = B_1 \cdot B_2 \cdot B_3 \cdot \bar{B}_1^* \cdot \bar{A} \cdot \bar{U}_2 \cdot \bar{D}_2 \cdot \bar{L} \cdot \bar{R},$$

$$K = [(U_1 \cdot U_2) \text{ or } (D_1 \cdot D_2)] (\bar{U}_1 \cdot \bar{D}_1) \cdot \bar{B}_1,$$

where B_1^* was B_1 2 μsec wide to reject events where the preceding beam particle was closer than 2 μsec , and L and R were partially overlapping counters at a beam focus downstream (not shown in Fig. 1) to reject noninteracting ^{16}O beam particles.

The event trigger required K in coincidence with a 75 nsec wide gate signal, delayed by 11 nsec, which was generated by B . This occurred when a

beam particle had interacted and a K^+ decayed 11 nsec or more after the target interaction. Each event trigger caused the wide gap spark chamber to be pulsed and the K^+ decay time to be digitized for photographic recording.

The wide gap spark chamber consisted of two 25.4 cm gaps with 0.0025 cm aluminum foil electrodes. Each event was photographed both in the direct view and the reflected top view; the photographs were scanned for tracks which appeared to originate from decay vertices outside the target. The event rate was approximately 1 per 10^5 B -logic pulses; camera film advance dead time of 750 msec limited data accumulation to one or two photographs per pulse.

A histogram of the distances of the vertex points from the center of the 7.5 cm thick polyethylene production target is shown in Fig. 2(a). The large peaks are attributable to nuclear interaction in the 0.025 mm Al spark chamber plates and 0.75 mm scintillation counter B_3 . The time distribution of the delayed pulses from the K^+ detector corresponding to the plate interaction events is shown in Fig. 3(a). The distribution falls more rapidly than would be expected for the 12 nsec K^+ mean life, and is the distribution of some spurious source of delayed pulses. Many of the events with vertex positions outside the plates must also be nuclear interactions. In order to separate many of these from hypernuclear decay events, the distribution of the number of forward prongs was examined for several subgroups of events, as shown in Fig. 4. The interactions in the scintillation counter and first plate had the broad prong distribution shown in Fig. 4(a). The events with vertices within the first spark cham-

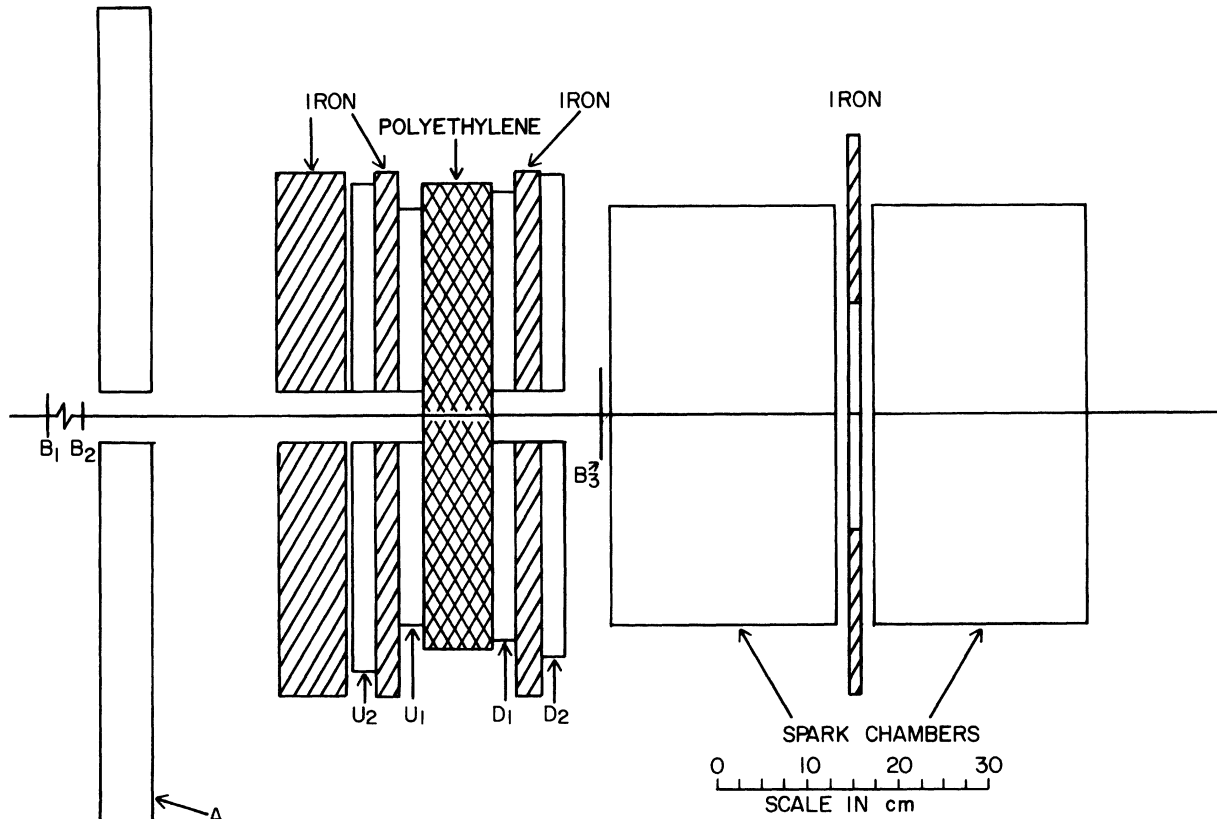


FIG. 1. Experimental layout.

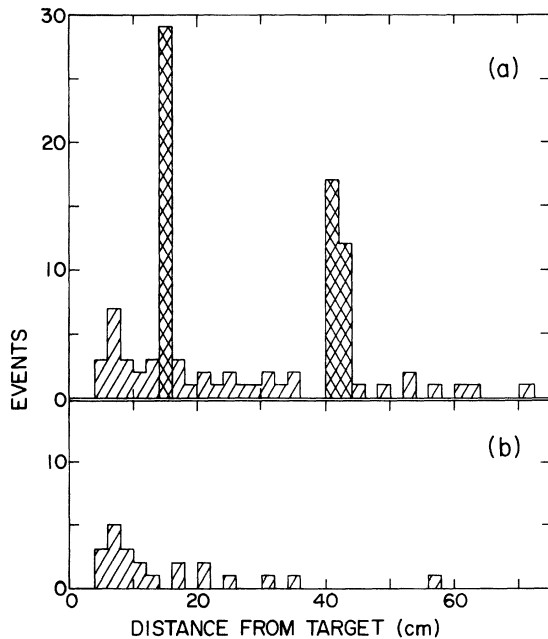


FIG. 2. Vertex distance distribution. (a) The distribution for all events. The large peaks are due to nuclear interactions in the spark chamber plates. (b) The distribution for 2, 3, and 4 prong events left after interactions in the plates have been removed.

ber gap are shown in Fig. 4(b). Finally, presumably the purest sample of hypernuclear decay events, those with vertices between the production target and the spark chamber, are shown in Fig. 4(c). The distribution in Fig. 4(c) appears appreciably narrower than the distribution for known nuclear interactions in Fig. 4(a), as expected for the comparatively small energy release in hypernuclear decay. On this basis, only events with vertices outside of plates with 2, 3, or 4 forward prongs were further considered. The decay distance distribution of these events is shown in Fig. 2(b), and the K^+ decay time distribution is shown in Fig. 3(b). Both distributions are consistent with attributing these events to the production and decay of hypernuclei.

The decay distance distribution can be fitted by a function of the form:

$$N(x)dx = (Ae^{-x/\lambda} + B)dx,$$

where λ is the mean decay length of the hypernuclei and the second term represents events due to nuclear interactions in the neon spark chamber gas, which should be uniformly distributed. Values of λ and B/A which best fit the 22 observed events were estimated by the maximum likeli-

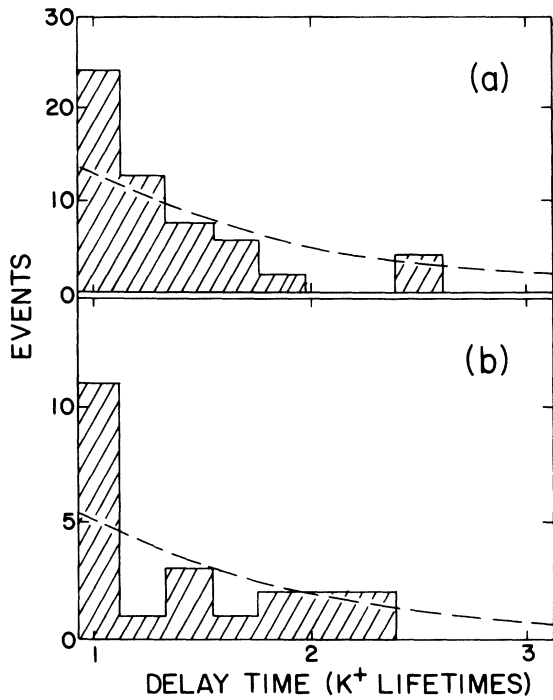


FIG. 3. K^+ decay time distribution (a) for background events, and (b) for events left after cuts have been applied. The dashed curves show the distribution expected for K^+ decay. The area under each curve has been normalized to the area of the histogram.

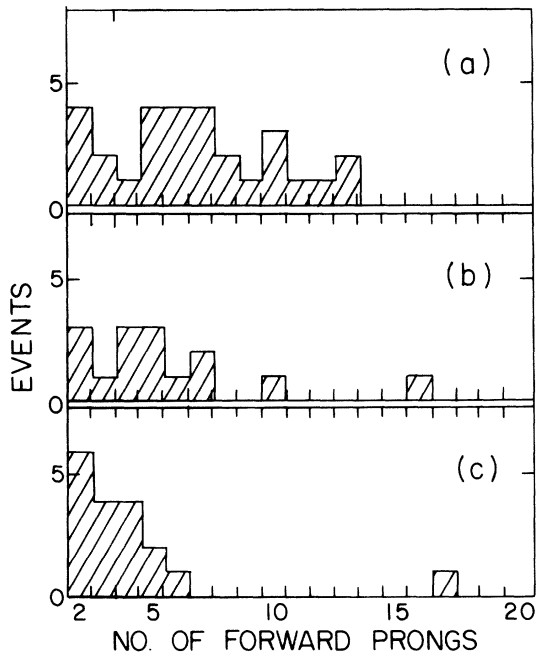
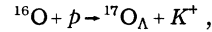


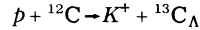
FIG. 4. Prong distribution. (a) Number of prongs for events in counter B_3 and first spark chamber plate. (b) Number of prongs for events in first spark chamber gap. (c) Number of prongs for events between target and spark chambers.

hood method to be $\lambda = 7.7_{-2.3}^{+3.0}$ cm and $B/A = 0.012_{-0.008}^{+0.016}$.

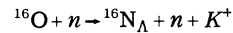
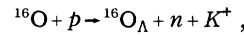
Production reactions with two body final states such as



were ruled out by the very small cross section upper limits obtained in a companion experiment where the reaction



was studied.² When the momentum transfer from incident heavy ion to outgoing hypernucleus is considered,³ reactions with three-body final states seem most likely for the production of hypernuclei. A Monte Carlo calculation of the reactions



was carried out. The three-body final states with a proton secondary were not included because they were rejected by the scanning criterion that no secondaries other than a high Z ion emanate from the polyethylene production target. The final state phase space was weighted by a factor $\exp[-q^2/2(m_\pi c)^2]$, where q is the three-momentum transfer between the incident ^{16}O and the outgoing hypernucleus, and $m_\pi c = 140$ MeV/ c is the pion mass. The results were not sensitive to other choices for the ^{16}O form factor. This calculation showed that $\beta\gamma$ of the hypernucleus should be sharply peaked with a mean value, $\langle\beta\gamma\rangle = 3.01$. If this value is used to convert the mean decay length to a lifetime, we find:

$$\tau(^{16}\text{Z}_\Lambda) = (0.86_{-0.26}^{+0.33}) \times 10^{-10} \text{ sec}$$

where $\tau(^{16}\text{Z}_\Lambda)$ represents the effective mean lifetime of the mixture of $^{16}\text{O}_\Lambda$ and $^{16}\text{N}_\Lambda$ produced in this experiment. This result is close to the life-

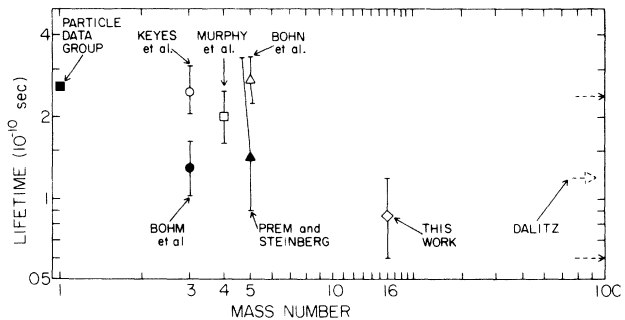


FIG. 5. Mean lifetimes of hypernuclei versus mass number (Refs. 4, 6-11). The points at masses 3, 4, and 5 refer to $^3\text{H}_\Lambda$, $^4\text{H}_\Lambda$, and $^5\text{He}_\Lambda$. The Dalitz point is a theoretical estimate for $A \approx 100$.

time prediction by Dalitz of 1.2×10^{-10} sec with an estimated uncertainty of a factor of 2 for Λ 's in heavy nuclei.⁴ The observed lifetime is shown in relation to the meager information on other measured hypernuclear lifetimes in Fig. 5.

If the above Monte Carlo calculation is used to evaluate the detection efficiency of the apparatus, a rough estimate of the cross section per target nucleon for hypernucleus production in association with a K^+ can be obtained:

$$\begin{aligned} \sigma(^{16}\text{O} + \mathcal{N} \rightarrow ^{16}\text{Z}_\Lambda + K^+ + \text{neutrons}) \\ = 2 \pm 1 \text{ } \mu\text{b}/\text{target nucleon.} \end{aligned}$$

For comparison, the total cross section for production of free Λ hyperons in 2.8 GeV proton-carbon collisions is⁵

$$\begin{aligned} \sigma(p + ^{12}\text{C} \rightarrow \Lambda_{\text{free}} + \text{anything}) \\ = 440 \pm 200 \text{ } \mu\text{b}/\text{incident proton.} \end{aligned}$$

The present arrangement yielded roughly one relativistic hypernucleus per hour of running with the beam intensity limited by spark chamber memory time and recovery dead time. Further optimization of the geometry, triggering scheme, and track detectors will permit study of hypernuclear properties, particularly decay modes and lifetimes.

We wish to thank Dr. H. H. Heckman and his colleagues for their assistance in utilizing their heavy ion beam at the Bevatron, Mr. Fred Lothrop and his staff for their usual efficient assistance, and Dr. E. P. Krider and Mr. P. Polakos for their timely help during the run.

*Work supported by National Science Foundation Grant No. MPS 70-02151.

‡Present address: AFWL/DYT, Kirtland Air Force Base, Albuquerque, New Mexico 87117.

†Present address: Argonne National Laboratory, Argonne, Illinois 60439.

¹H. A. Grunder, W. D. Hartsough, and E. J. Lofgren, *Science* **174**, 1128 (1971); H. H. Heckman, D. E. Greiner, P. J. Lindstrom, and F. S. Bieser, *Phys. Rev. Lett.* **28**, 926 (1972).

²T. Bowen, D. A. DeLise, and A. E. Pifer, *Phys. Rev. C* (to be published).

³V. N. Fetisov, M. I. Kozlov, and A. I. Lebedev, *Phys. Lett.* **38B**, 129 (1972).

⁴R. H. Dalitz, in *Proceedings of the International Conference on Hyperfragments*, St. Cergue, March 1963 [CERN Publication No. 64-1, 1964, (unpublished)], p. 147; and in *Proceedings of the Conference on Nuclear and Hypernuclear Physics with Kaon Beams*, Brookhaven National Laboratory, July 1973 [BNL Report No. 18335 (unpublished)], p. 1.

⁵T. Bowen, J. Hardy, Jr., G. T. Reynolds, G. Tagliaferri, A. E. Werbroeck, and W. H. Moore, *Phys. Rev.* **119**, 2041 (1960).

⁶Particle Data Group, *Phys. Lett.* **50B**, No. 1 (1974).

⁷G. Keyes, J. Sacton, J. H. Wickens, and M. M. Block, *Nucl. Phys.* **B67**, 269 (1973).

⁸G. Bohm, J. Klabuhn, U. Krecker, F. Wysotzki, G. Coremans, J. Sacton, P. Vilain, J. H. Wickens, G. Wilquet, D. O'Sullivan, D. Stanley, D. H. Davis, T. Pniewski, T. Sobczak, and J. E. Allen, *Nucl. Phys.* **B16**, 46 (1970).

⁹C. T. Murphy, T. Church, J. Morfin, H. Ring, and L. Fortney, in *Proceedings of the International Conference on Hypernuclear Physics*, Argonne National Laboratory, May 1969 (unpublished), p. 438.

¹⁰G. Bohm, J. Klabuhn, U. Krecker, F. Wysotzki, G. Bertrand-Coremans, J. Sacton, J. Wickens, D. H. Davis, J. E. Allen, and K. Garbowska-Pniewska, *Nucl. Phys.* **B23**, 93 (1970).

¹¹R. J. Prem and P. H. Steinberg, *Phys. Rev.* **136**, B1803 (1964).